

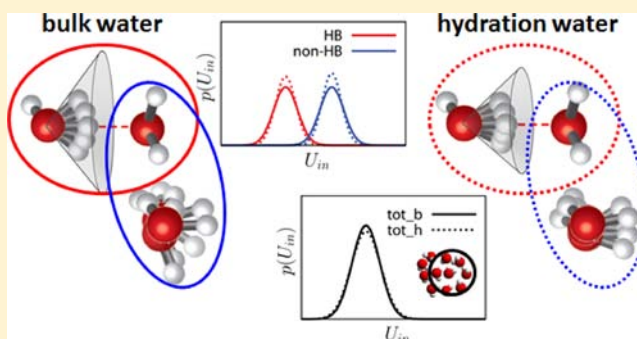
Physical Origin Underlying the Entropy Loss upon Hydrophobic Hydration

Aljaž Godec* and Franci Merzel*

National Institute of Chemistry, Hajdrihova 19, 1000 Ljubljana, Slovenia

S Supporting Information

ABSTRACT: The hydrophobic effect (HE) is commonly associated with the demixing of oil and water at ambient conditions and plays the leading role in determining the structure and stability of biomolecular assembly in aqueous solutions. On the molecular scale HE has an entropic origin. It is believed that hydrophobic particles induce order in the surrounding water by reducing the volume of configuration space available for hydrogen bonding. Here we show with computer simulation results that this traditional picture, based on average structural features of hydration water, configurational properties of single water molecules, and up to pairwise correlations, is not correct. Analyzing collective fluctuations in water clusters we are able to provide a fundamentally new picture of HE based on pronounced many-body correlations affecting the switching of hydrogen bonds (HBs) between molecules. These correlations emerge as a nonlocal compensation of reduced fluctuations of local electrostatic fields in the presence of an apolar solute. We propose an alternative view which may also be formulated as a maximization principle: The electrostatic noise acting on water molecules is maximized under the constraint that each water molecule on average maintains as many HBs as possible. In the presence of the solute the maximized electrostatic noise is a result of nonlocal fluctuations in the labile HB network giving rise to strong correlations among at least up to four water molecules.



INTRODUCTION

The hydrophobic effect (HE) has a multifaceted nature, i.e., its physical manifestation depends on the length scale.¹ On the mesoscale, i.e., hydration of an assembly of hydrophobic units or an extended hydrophobic surface, HE is driven by energy/enthalpy and occurs as a “dewetting” transition^{2–4} which has far-reaching consequences for processes, such as protein folding^{5,6} and nanoparticle self-assembly.⁷ Meanwhile, HE on the molecular scale has an entropic origin,^{1,8,9} particularly near room temperature and lower, while it is believed to eventually become energy/enthalpy driven at higher temperatures.^{10,11} Furthermore, the molecular scale hydration thermodynamics (hydrophobe solubilities, partitioning of hydration free energy into energy/enthalpy and entropy contributions, etc.) appear to be well established and can be worked out, for example, using scaled particle theory¹² or information theory.¹³ While those theories are successful in predicting solubilities of hydrophobic solutes and several related thermodynamic features, they do not provide deeper insight into the physical mechanism underlying HE. Notwithstanding all efforts and advances in the field^{1–4,8,12,14–16} the physical picture of HE is still far from being complete and even fundamental issues, such as the mechanism underlying hydrophobicity on different length scales, still have to be clarified. From the physical point of view the most puzzling feature of HE remains the microscopic picture of entropy loss upon hydrophobic hydration.

Intuitively, the entropy loss is usually attributed to the reduction of configuration space available for hydrogen bonding,^{1,8,9} which is due to the fact that water molecules need to reorganize around a hydrophobic solute to avoid sacrificing hydrogen bonds (HBs). This is supposed to lead to remnants of clathrate structures¹⁷ which are, however, not rigid, and their quantitative importance for understanding hydrophobicity remains questionable.¹⁶ Furthermore, even the actual role of HBs for the HE is apparently not entirely clear.^{11,18} Thus, the physically most intriguing question to be answered still remains: If HE is entropy driven, what specifically causes the loss of entropy? Since entropy loss is directly related to a reduction of available volume in configuration space, how does it affect degrees of freedom of water molecules?

Here we present compelling simulation results which unravel a fundamentally new picture of the mechanism of HE based on pronounced many-body correlations affecting the intermolecular exchanging of HBs. We carry out constant pressure Monte Carlo simulations of TIPSP¹⁹ and SPC/E²⁰ water models and model hard sphere solutes in an orthogonal simulation box with periodic boundary conditions.

Received: July 3, 2012

Published: September 24, 2012

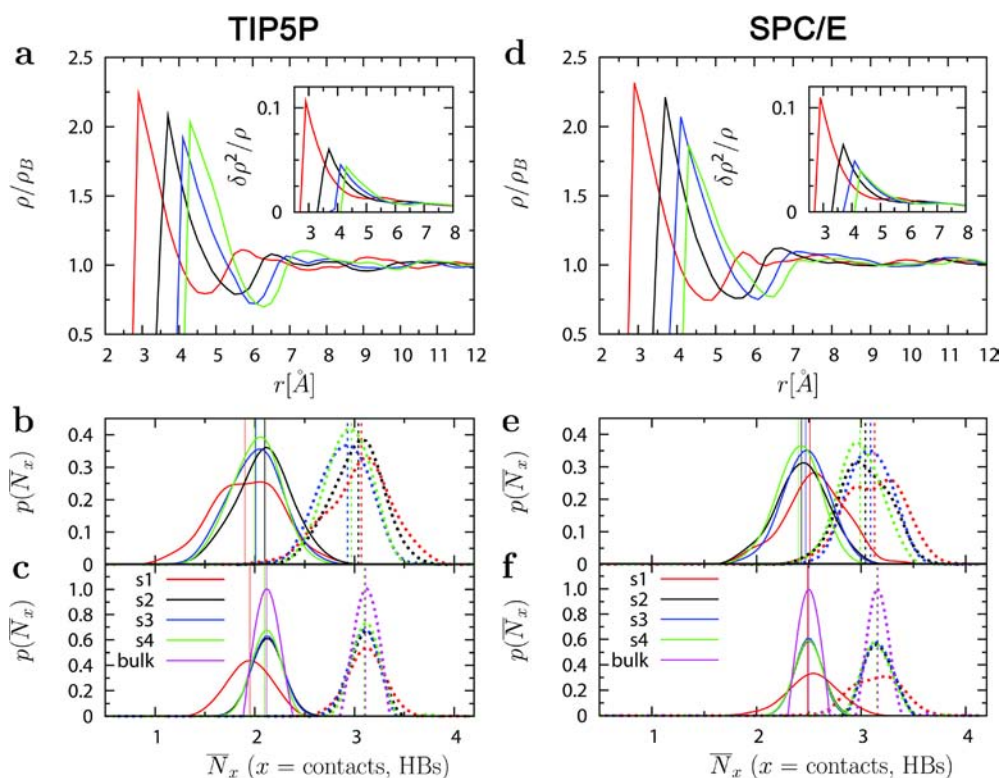


Figure 1. Radial ordering around hydrophobic particles: (a,d) Radial correlation function for TIP5P and SPC/E water centers; (inset) corresponding relative density fluctuations. (bottom) Distribution of the number of total (dashed lines) and hydrogen-bonded (full lines) contacts per water molecule located in (b,e) first and (c,f) second hydration shells, with the corresponding bulk water values for comparison. The vertical lines denote expected values. The solute sizes are: $r(s1) = 1.4$, $r(s2) = 2.1 (= 1.5 \times r_{\text{H}_2\text{O}}^{\text{hs}})$, $r(s3) = 2.52 (= 1.8 \times r_{\text{H}_2\text{O}}^{\text{hs}})$, and $r(s4) = 2.8 (= 2 \times r_{\text{H}_2\text{O}}^{\text{hs}})$ Å (see Methods section for details).

METHODS

We performed extensive constant pressure Monte Carlo (MC) simulations with TIP5P and SPC/E water and freely moving hard sphere solutes at room temperature (298 K) and 1 atm, assuming periodic boundary conditions. After an extensive equilibration period we performed as many trial moves as to ensure that on average each molecule was successfully moved 4×10^5 times at the maintained acceptance rate of 30%. To exclude (auto)correlations, the successive configurations used for the analysis were taken to be as far apart as to ensure that between each taken configuration each molecule was successfully moved at least five times. The hard sphere radius of the water molecule when in close contact with the hydrophobic spheres was taken to be 1.4 Å. The following radii of solutes were considered: $r(s1) = 1.4$, $r(s2) = 2.1$ ($1.5 \times r_{\text{H}_2\text{O}}^{\text{hs}}$), $r(s3) = 2.52$ ($1.8 \times r_{\text{H}_2\text{O}}^{\text{hs}}$), and $r(s4) = 2.8$ ($2 \times r_{\text{H}_2\text{O}}^{\text{hs}}$) Å. According to the solute size the number of water molecules was (in ascending size) 2668, 2670, 3513, and 3560. The total number of MC steps was 35.57×10^8 , 35.60×10^8 , 46.8×10^8 and 47.5×10^8 .

Inconsistencies of the Traditional Picture. In order to present the conceptual change in our understanding of the HE we first address the inconsistencies of the traditional picture. The term traditional picture represents the view on hydrophobic hydration that focuses on average structural features of hydration water and on properties of single water molecules and up to pairwise correlations. The radial correlation function, $(\rho(r))/(\rho_B) \equiv g(r) = \rho_B^{-1} \langle \sum_{i=1}^N \delta(r-|r_i|) \rangle$, is used to quantify the degree of translational ordering of water molecules around hydrophobic solutes. In the case of TIP5P water, we find a nonmonotonic dependence of the contact density on particle size, which is due to commensurability of the solute surface and water packing. In the case of SPC/E, water the contact density decreases monotonically with solute radius. The relative density fluctuations monotonically decrease with solute size for both water models

considered, and they are overall more pronounced in SPC/E water. As a result of solute–solvent dispersion interactions the monotonicity of relative density fluctuations continues as the solute size grows further to dimensions of nanodroplets.²¹ On the molecular scale (of main interest in the present work) the monotonicity is most likely a consequence of the fact that even constant relative density fluctuations would demand increasingly cooperative molecular rearrangements in the hydration shells, which would be entropically strongly disfavored. Two water molecules are defined to be in close contact if their intermolecular distance is less than 3 Å, and they are said to be hydrogen-bonded if they are in close contact and if the angle O–H...O is larger than 150°. The cutoff distance for neighbors in close contact is set at 3 Å and is more appropriate with respect to the conventional definition of 3.5 Å,²² as there is no preferential mutual orientation beyond the distance of 3 Å (see Figure 2c). The distribution of the number of water molecules in close contact and the number of hydrogen-bonded contacts per water molecule located in the first and second hydration shell and in bulk water are shown in Figure 1b,e and c,f, respectively. Except for the smallest solute in the case of TIP5P water (with radius 1.4 Å) there is no appreciable difference (say of the order of 0.5) in the number of total and hydrogen-bonded contacts with respect to bulk water, neither in the first nor in the second hydration shell. If the main effect of a hydrophobic solute would be the reduction of the configuration space for hydrogen bonding, then one would naturally expect to find less neighbors in close contact. Clearly, this is not the case. Moreover, the distribution is much narrower in bulk water, which already suggests that the small-scale fluctuations in the vicinity of hydrophobes (i.e., librations, HB exchange, etc.) are enhanced with respect to the bulk. According to our criterion for the nearest neighbor, we find that the probability of a water molecule having three hydrogen-bonded nearest neighbors is negligible, irrespective of its position. By comparing the results for TIP5P and SPC/E models, we find that SPC/E water tends to form slightly more

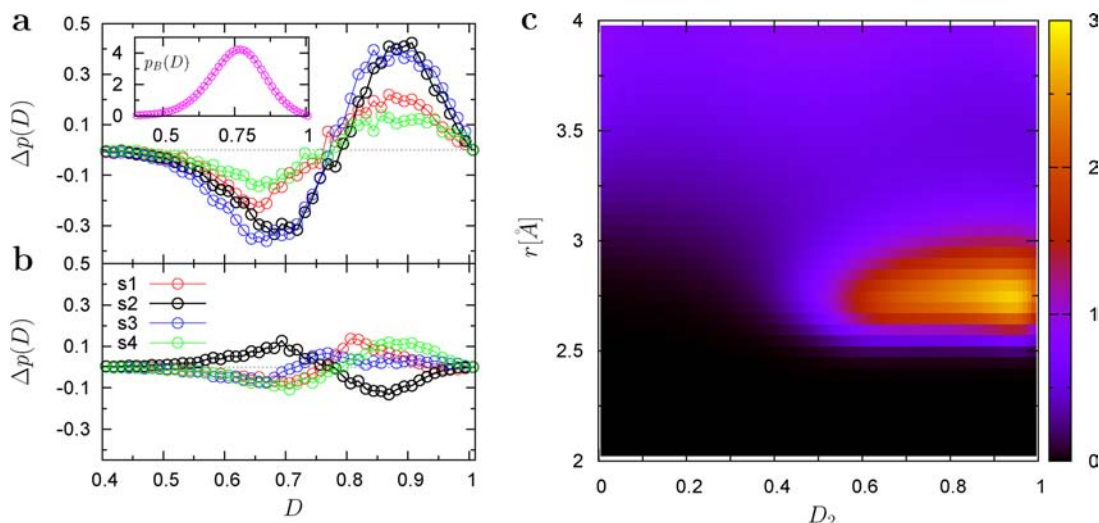


Figure 2. Mutual orientational ordering of TIPSP water molecules in close contact: Difference in the distribution of the dipolar order parameter with respect to the bulk, $\Delta p(D) = p(D) - p_B(D)$, in the (a) first and (b) second hydration shells. Inset of (a): The dipolar order distribution in bulk water is shown. (c) Joint probability of finding two molecules at a distance r apart having a (pair) mutual order D_2 (see eq 1 for definition, with $N = 1$).

HBs (2.5 compared to 2.1 in the case of bulk TIPSP) both in the bulk phase as well as in the hydration shells, while the total number of nearest neighbors is the same in both cases.

Aside from an altered number of nearest neighbors, the traditional picture also suggests a more ordered local structure. In order to cause entropy loss the structural fluctuations should tend to diminish. To inspect in detail the structural ordering of water molecules in close contact, around hydrophobic particles, and in bulk water, we employ the recently introduced dipolar order parameter:²³

$$D(i) = \frac{1}{N} \sum_{j=1}^N \left(\frac{\alpha_{ij} - \alpha_{ij}^{\min}}{\alpha_{ij}^{\max} - \alpha_{ij}^{\min}} \right) \quad (1)$$

where $i \neq j$ and the sum is taken over the N neighbors in the first coordination shell of the i -th water molecule and α_{ij}^{\max} and α_{ij}^{\min} correspond to maximal and minimal dipole–dipole potential at a given intermolecular unit vector and unit dipole vector of the tagged molecule. This way, $D(i)$ takes values between 0 (maximal repulsion) and 1 (maximal attraction). The distributions of dipolar ordering in the case of TIPSP shown in Figure 2 confirm the idea that water is on average slightly more orientationally ordered in the first hydration shell of hydrophobic particles (note the slight shift of the distributions toward higher D values). More importantly, the width of the distributions $p(D)$, which reflects the constraining of orientational degrees of freedom, remains rather unaffected. This width clearly increases upon increasing polarity of the solute indicating an orientational relaxation in the HB network.²³ The situation in the second shell is similar, albeit less pronounced. Most likely, due to a commensurability effect, the second shell molecules exhibit a reverse trend in orientational ordering in the case of s2. The results in the case of SPC/E are essentially the same, except that bulk SPC/E water is intrinsically slightly less ordered as compared to bulk TIPSP (see Figure 1 in the Supporting Information).

Apparently the pair interactions and consequently also the HBs are strengthened, but there is no reduction of the orientational configuration space explored by individual water molecules in the hydration shells as the distributions are merely shifted, while their form remains unchanged. Thus, we find that (i) there are no significant differences in the number of nearest HB and non-HB neighbors and (ii) there is no orientational constraining although the local structure is more ordered. Similar results of (i) based on both experiments as well as simulations have already been reported previously.^{24–30} This is clearly in contradiction with the idea of reduced configuration space available for hydrogen bonding.^{1,8,9} So how can this contradiction be reconciled?

An Alternative View: Emergence of Many-Body Correlations.

There is an important difference between the total volume of configuration space and the volume that is actually visited at a given temperature. As the number of close contacts is not altered significantly by the mere presence of the solute, the latter is not expected to significantly affect the volume of the configuration space available to a water molecule for hydrogen bonding. On the other hand, in the liquid state water molecules form a dynamic, labile HB network. There is clear evidence that the molecular reorientation underlying the exchange of HBs is not diffusive (i.e., does not occur as angular Brownian motion) but rather proceeds in terms of large-amplitude sudden jumps.^{22,31–37} As it is impossible for water molecules to each form four HBs at a time in the liquid state, this introduces a strong frustration into the system emerging from the competition between the entropic and the energetic driving forces. This means that while fluctuating about the minimum energy configuration exhibiting, for example, librational movements, a water molecule is most likely to form two HBs to its closest neighbors. As a water molecule in the bulk liquid is intrinsically inclined to form more than one HB, this necessarily leads to confinement of its orientational configuration space. This fact suggests to rationalize the entropy loss in HE in an alternative way.

The current understanding of HB network dynamics in bulk water already anticipates the existence of collective effects involving several water molecules and an immediate reorganization of the HB network upon an exchange event.^{36,37} This suggests looking for the potential source of entropy loss in the altered “communication” between emerging transient water clusters involved in the exchange of HBs, i.e., the reduction of configuration space due to constraining of collective degrees of freedom. For large enough fluctuations the transient water cluster can rearrange into another configuration just by the exchange of HBs. Hydrogen-bond fluctuations (for example, librations) try to compensate for the entropic frustrations caused by a transient mutual alignment of water molecules in between sudden jumps. Since structural fluctuations are caused by local field fluctuations, they are expected to be dramatically suppressed in direct vicinity of a hydrophobic solute, because the latter exerts only an extremely weak electrostatic field. Without an additional compensation mechanism the HBs would be significantly strengthened, and the entropic frustrations would be expected to grow further. Therefore there must exist a tendency of nearby water molecules (nearest and next-nearest neighbors) to compensate for the suppressed fluctuations of local electrostatic fields. This in turn can not happen unless the fluctuations of nearby hydrogen-bonded clusters (intra- and intercluster fluctuations) become correlated as to maximize local field fluctuations while

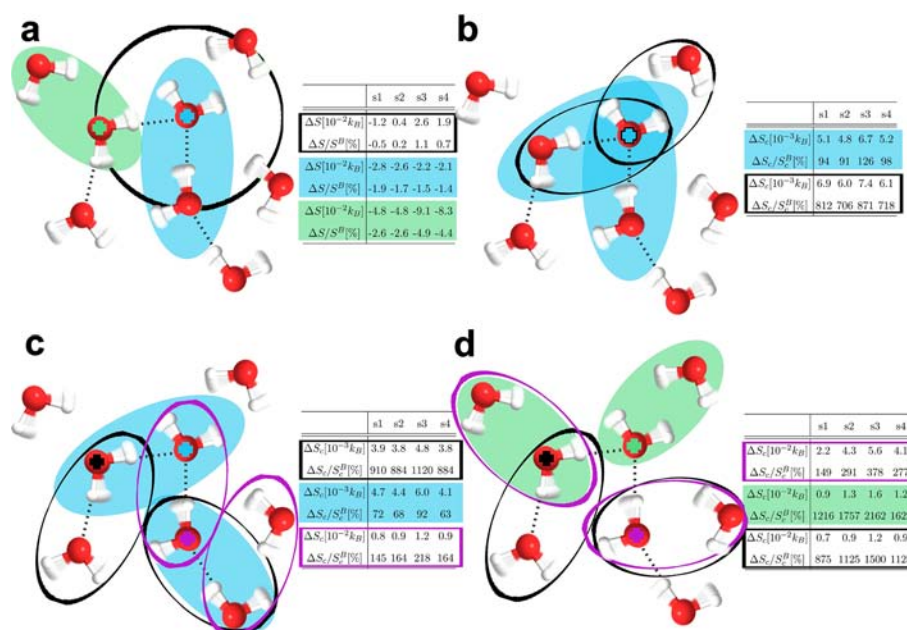


Figure 3. Fluctuation and correlation entropy differences per tagged pair/cluster in the first hydration shell with respect to the bulk are given in the tables. Correlations between differently interacting pairs of water molecules are depicted by color in schematics and Tables. Only the tagged molecule necessarily lies in the first hydration shell. The “+” denotes the tagged molecule which is used for the localization of a given cluster, and the dashed black lines denote HBs. The results are given for the TIPSP water model. (a) Absolute and relative entropy difference of fluctuations of HB (blue shading) and non-HB (green shading) and total interaction energy with nearest neighbors (black frame). (b) Three-body correlation entropy of geminal (pairs share the tagged molecule) HB pairs (blue shading) and a geminal HB and non-HB pair (black frame). Four-body correlation entropy of HB-bridged HB (blue shading) and non-HB-bridged HB (black frame) pairs and a vicinal (pairs do not share the tagged molecule) tagged HB and non-HB pair (magenta frame). (d) Four-body correlation entropy of vicinal HB-bridged non-HB (green shading), vicinal non-HB-bridged non-HB (magenta frame), and vicinal tagged non-HB and HB (black frame) pairs.

maintaining as many as possible mutual water arrangements close to the optimal HB geometry. Thus, in order to satisfy the local energetic demand to form HBs, the resulting entropic frustration relaxes nonlocally in the vicinity of a hydrophobic solute.

Testing this hypothesis demands the evaluation of various many-body correlations and their role in lowering the systems entropy. Thereby it is rather inconvenient to pertain to the classical Boltzmann view on the entropy, which essentially deals with the number of microscopic states of a single system, and according to which, entropy is an additive quantity. In our particular problem we are interested in entropy changes within the hydration shell such that our subsystem is smaller than the correlation length, and hence the entropy of individual constituents of the subsystem is not equal to the sum of entropies. Instead we adopt the view to interpret entropy in terms of uncertainty. Namely, due to thermal fluctuations of molecules the exact state of a subsystem of interest (for example, of the first hydration shell) is uncertain, and the larger the uncertainty the larger is the entropy. In absence of any correlations the (excess) entropy of molecules in the hydration shell would be equal to the number of molecules in the shell times the entropy of a single molecule. The latter would be defined as the uncertainty of coordinates of single molecule. Hence the hydration entropy would represent the difference of uncertainties in the presence and absence of the solute. If a decreased volume of the configuration space available to a water molecule for hydrogen bonding would be responsible for the entropy loss upon hydration, the latter difference in uncertainties would represent the leading order effect.

Any correlation decreases the total uncertainty and leads to violation of additivity of entropy. Meaning that the total excess entropy is in fact the sum of single molecule uncertainties diminished by all possible correlation terms, $S_{\text{ex}} = NS_1 - \sum_i \alpha_i S_i^C$, where α_i takes into account the number of distinct terms of the same order. Being focused on molecules within the hydration shell we would traditionally be forced to evaluate a series of N -body entropies, $S_{\text{ex}} = S^{(1)} + S^{(2)} + \dots$, represented by integrals of nonlocal many-body correlation functions

over molecular coordinates (see ref 38), which would present a formidable computational task.

Although addressing the problem of coupled translational–orientational multibody correlations is nontrivial, it can be significantly simplified in the following manner. While single water molecules are, by nature, indistinguishable, they can be transiently classified as being hydrogen bonded or nonbonded to its nearest neighbor (using the same criteria as above). Any HB exchange event merely permutes the indices between water molecules. With these criteria we can, at any instant, classify the HB and non-HB neighbors of any given molecule. Involving various types of fluctuations on different time scales, such as librations, dimer tumbling, and HB jumping (see ref 36 and references therein), following both the relative positions and orientations of water molecules individually is simply too complex and in fact unnecessary. To determine how molecular degrees of freedom are constrained in the liquid state, we shall be primarily interested in structural fluctuations in water clusters. Such fluctuations can be easily described in terms of fluctuations of interaction energies of hydrogen bonded and non-hydrogen bonded molecules.

Using the random variable transformation theorem³⁹ we can map the joint configurational probability density onto its functionally dependent joint probability density for pair potential energies. Thereby a given matrix of molecular positions and orientations, Ω , is mapped onto a vector of interaction energies, U , which can be formally written for given values ω and u as follows

$$p(u) = \int d\omega^N P(\omega^N) \delta(u - f(\omega^N)) \quad (2)$$

The functional relation $\delta(u - f(\omega^N))$ contains a class indicator (close contact, hydrogen-bonded, etc.) as well as the appropriate averaging operation accounting for the indistinguishability of pairs within a certain class (for details see Supporting Information, Section 1). This way we can construct, using appropriate functional relations, probability densities for observing, for example, a (non)hydrogen bonded pair with certain energy or a joint probability density of

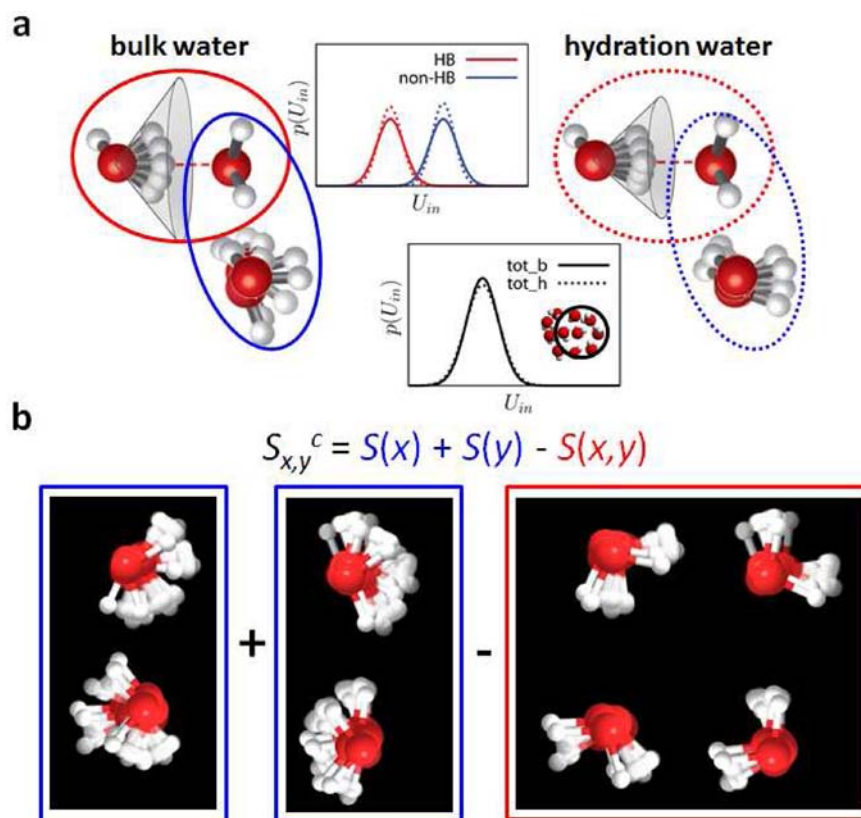


Figure 4. Fluctuations and many-body correlations. (a) Schematic of distribution of potential energies of hydrogen (red) and non-hydrogen (blue) bonded interactions along with the distribution of potential energies of total interactions with neighbors in close contact (black). (b) Schematic illustration of the meaning of the four-body correlation entropy. Full lines denote values in bulk water and dashed lines those in hydration water.

observing two pairs of different classes having given energies. Comparing the values per water molecule/cluster inside the first and second hydration shells with the corresponding bulk values we are able to select the most important contributions to the entropy loss. The Gibbs–Shannon entropy, $S[p] = -k_B \int p(u_i) \ln p(u_i) du_i$, is used to evaluate the total uncertainty of a quantity u_i and thus quantifies the fluctuations. Alternatively, Kullback–Leibler entropy or correlation entropy (the latter is taken after)⁴² is used to quantify the total correlation between two random variables X and Y (which can be components of U , for example, various combinations of HB and non-HB pairs (U_{HB} and U_{non-HB})). The correlation entropy can be expressed in terms of individual and joint entropies, $S_C(X,Y) = S(X) + S(Y) - S(X,Y)$ or explicitly in terms of corresponding probability densities:

$$S_C(X, Y) = k_B \iint p(x, y) \ln \frac{p(x, y)}{p(x)p(y)} dx dy \quad (3)$$

We limit the present discussion to three- and four-particle correlations to assess how fluctuations of various HB and non-HB pairs are correlated. The difference of fluctuation and correlation entropies of a given type in the hydration shell and in bulk water will serve as a measure for the role of a given fluctuation/correlation in lowering the excess entropy. The resulting entropies are, however, not in 1 to 1 correspondence with the thermodynamic N -body entropies in the traditional correlation expansion.³⁸

Being predominantly interested in generic features and less on the specific effect of solute sizes, we focus first on the properties of individual pairs of molecules and find that the dipolar entropy difference between the hydration shells and the bulk, which directly measures the degree of orientational constraining, does not show a monotonic behavior with respect to the solute size and is less than 1% of the corresponding bulk value for both water models considered (for details see Supporting Information, Section 3). (To avoid duplication of information Figure 3a contains results for the TIPSP model only.

The results for the SPC/E model are given in the Supporting Information, Table 2.) This confirms the assumptions that a reduced orientational configuration space of single molecules is not the reason for HE. This fact is further substantiated with the values of the entropy difference, ΔS_{tot-C} , of the fluctuations of the total interaction energy of tagged molecules with its nearest neighbors, $S[p(\sum_i U_{i0})]$, (Figure 3a). It may also be taken as a contribution to the fluctuations of the local electrostatic field (solely) due to the thermal motion of nearest neighbors. In fact, ΔS_{tot-C} is mostly positive, except for the smallest solute which indicates that local field fluctuations due to nearest neighbors are enhanced in the vicinity of the hydrophobe. Meanwhile, the entropy of mutual fluctuations of the potential energy of both hydrogen-bonded neighbor pairs (Figure 3a, blue) and non-hydrogen-bonded pairs (Figure 3a, green) decreases with respect to bulk water. The former can be understood as a measure of librational-type of fluctuations, and its lowering is indicative of a slight HB strengthening³⁴ (though the relative difference is smaller than 2% of the bulk value). Together with decreasing fluctuations of the non-HB interaction energy and the simultaneous increase of fluctuations of the total interaction energy with nearest neighbors, this immediately hints at higher order (beyond pair) correlations, as suggested by our hypothesis (see schematic in Figure 4a). The local strengthening of HB is also suggested by the shift of $p(D)$ toward larger D . The fact that fluctuations of the total interaction energy are so small and their entropy difference mostly even positive along with the strengthening of HB are fully consistent with the existence of sudden jumps in HB-network dynamics. A closer look at entropies of various three- and four-body correlations in Figure 3b–d reveals striking, up to 22-fold increases with respect to bulk water. The largest increase is observed in the case of correlations of nearby non-HB pairs bridged via a HB (12–22 fold), a HB pair and a nearby non-HB pair (7–9 fold, 9–15 fold in the case of geminal, and 9–15 fold in the case of vicinal pairs), and two HB pairs that do not share a common HB bond (are not bridged via a HB; 9–11 fold). A significant, albeit smaller, increase is also observed

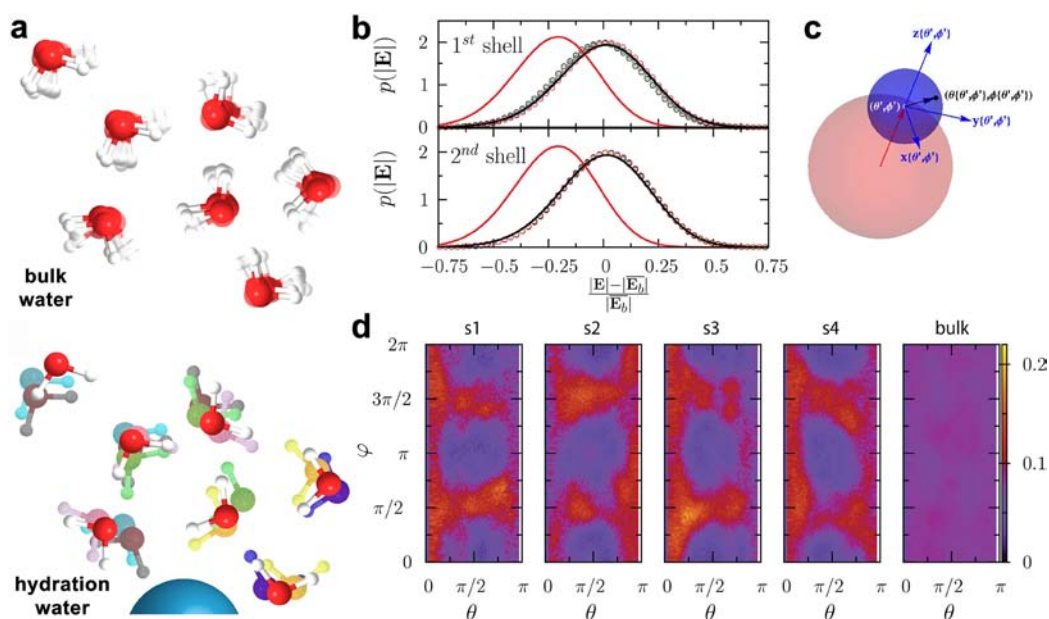


Figure 5. Emergence of pronounced many-body correlations and their physical origin in the case of TIP5P water. (a) Schematics of predominantly pairwise correlated fluctuations in bulk water and emerging many-body correlations in the hydration shell. Different colors denote various orders of correlated fluctuations. (b) Distribution of magnitudes of the local electrostatic field experienced by a water molecule at a given location. Black lines denote distributions in bulk water and symbols represent results for water molecules around apolar solute. If one nearest-neighbor water molecule is omitted from the calculation of the local field in the bulk, this leads to uncompensated fluctuations shown by the red distribution. (c) The coordinate frame used in the calculation of angular distributions of local electrostatic fields. (d) Distribution of orientations of the local electrostatic field in the first hydration shell of apolar solutes and in bulk water.

in the case of geminal HB pairs ($\sim 100\%$ increase) and HB pairs which are bridged via a HB (70–90% increase). Let us briefly mention that all three- and four-body correlations are, to linear order, anticorrelated. The pronounced many-body correlations propagate into the second hydration shell (for details see Supporting Information, Section 3, Table 1) but fall off rapidly further away. Thus, the picture of two perturbed hydration layers is retained. For an illustration of the general physical meaning of many-body correlations in the present context see Figure 4b. The results for the SPC/E model are essentially very similar, but the increase of many-body correlations is even more pronounced (for details see Supporting Information, Table 2). It is interesting to note that comparing many-body correlation entropies in bulk SPC/E and TIP5P water, the correlations between non-HB pairs (geminal and vicinal) are found to be stronger in bulk SPC/E, while correlations between HB pairs as well as between a HB and a non-HB pair are found to be weaker in bulk SPC/E. This can be attributed to the fact that TIP5P intrinsically slightly over favors tetrahedral configurations with respect to SPC/E. Note that the many-body correlations discussed above are essentially captured in fundamental thermodynamic quantities referred to in ref 40 as the solvent reorganization entropy and solute–solvent fluctuation entropy.

Our findings are conceptually compatible with the results of Irudayam and Henchman,⁴¹ who also reported on the complete absence of single water molecule confinement but suggested that the entropy loss is due to a lower number of ways the whole HB network can form. They, however, assumed a static and highly idealized local structure of HB clusters, neglected all correlations between adjacent HB clusters, and consequently attributed the entropy loss specifically to a decreased number of orientational minima per water molecule in the vicinity of the solute. Nevertheless, since the existence of many-body correlation effectively decreases the actual number of distinct configurations of the HB network, their view might be seen as to be in conceptual agreement with the present results.

Microscopic Physical Origin of the Entropy Loss. The results suggest that the traditional explanation of the HE on the molecular scale needs a substantial revision. It is not a reduced configuration space for hydrogen bonding that is responsible for the observed lowering of entropy, but a striking increase of many-body correlations

(Figure 5a), which is essentially due to hydrogen bonding being a strong and orientationally dependent interaction. The increase of many-body correlations is necessary to compensate for the reduction of fluctuations in the local electrostatic field and the resulting local HB-strengthening when one or more “polar” water molecules are replaced by an “apolar” hydrophobic particle. This effect should scale as the difference between local field distributions experienced by the water molecule in bulk (Figure 5b, black curve) and by a bulk water molecule for which one neighboring water molecule is omitted from the calculation of the local field (Figure 5b, black curve). Results are given as relative deviations from the average bulk value $\langle |E| \rangle$. If left uncompensated, such as in the case when one neighboring water molecule is omitted from the calculation, the distribution is shifted significantly to lower values. It also turns out that the distributions of field strengths in the hydration shells are almost identical to the one in bulk liquid (Figure 5b, symbols).

The distribution of orientations of the instantaneous electrostatic field can be effectively investigated by introducing a secondary coordinate frame (Figure 5c), constructed in the following manner (also see Supporting Information, Section 3). The radial projection of the water molecule position onto a spherical surface (θ', φ') defines the origin and orientation of a secondary coordinate system (blue), such that the secondary $z(\theta', \varphi')$, $x(\theta', \varphi')$, and $y(\theta', \varphi')$ axes correspond to the local radial, polar, and azimuthal directions. The angular coordinates in the secondary frame $(\theta\{\theta', \varphi'\}, \varphi\{\theta', \varphi'\})$ are then used to describe the distribution of the local field over the surface of the unit sphere.

By looking at the distribution of orientations of the local field over the unit sphere shown in Figure 5d we find that the distribution is isotropic in the bulk as well as in the second hydration shell (see Supporting Information, Figure 2). Meanwhile, in the first hydration shell the local field fluctuations are constrained to the plane containing the normal to the solute surface. Such a distribution ensures that all water molecules in the first hydration shell experience the maximum span of local fields and thereby local torques which counteract the entropic frustrations caused by a transient mutual alignment of water molecules in between HB exchange events. Such a compensation mechanism comes at cost of many-body correlations. The local

increased entropic frustration is thus compensated nonlocally. The same results are obtained for SPC/E water (see Supporting Information, Figure 3), readily demonstrating that our general view is qualitatively insensitive to the parameters of the force field.

CONCLUSION

The proposed picture of hydrophobic hydration does not imply any water immobilization in the spirit of the iceberg hypothesis. In explaining the retardation of reorientation dynamics^{28,29,33,43,47} the current picture, based on the excluded volume effect, proposes that the slowdown is a result of fewer accessible configurations of the transition-state (TS) in a HB exchange event due to the presence of the solute. While our analysis is focused on fluctuations in the HB network in equilibrium and thus cannot directly challenge the view on dynamics of water reorientation, our results nevertheless suggest that slower water reorientation in the vicinity of the solute could alternatively also be explained by increased many-body correlations (due to correlations the TS is simply statistically less probable) rather than actual sterical hindrance of reorientation. Inasmuch as the actual HB exchange event is caused by an instantaneous electric field fluctuation of a critical magnitude to break a HB and reorient the molecule to form a new bond, the probability of the occurrence of such a critical fluctuation should be smaller in the vicinity of the apolar solute due to the existence of increased many-body correlations. Such an alternative view might be beneficial considering that according to recent ab initio simulations³⁷ instantaneous overcoordination and defects, which are thought to be vital in the reorientation mechanism, are caused by a complex and highly fluctuating HB network. Our view also provides an explanation of the slightly better solubility of nonpolar solutes in heavy relative to light water.⁴⁴ While being more inert, heavy water responds less strongly to local field fluctuations, which leads to HB strengthening and thus a higher cohesive energy density⁴⁴ and also results in a more structured liquid with respect to light water.⁴⁵ Being intrinsically more structured the relative extent of local field fluctuations to be compensated upon the introduction of a hydrophobic molecule is therefore also smaller.

The results allow us to speculate that the range of hydrophobic interactions beyond that expected from the minimally exposed surface area reasoning is a result of the propagation of many-body correlations beyond the first hydration shell. Finally, we note that it should also be interesting to apply the correlation analysis presented here to the study of general features of hydration phenomena, such as ion hydration, in particular the local asymmetry of the hydration environment reported in.⁴⁶

ASSOCIATED CONTENT

Supporting Information

This material is available free of charge via the Internet at <http://pubs.acs.org>.

AUTHOR INFORMATION

Corresponding Author

franci.merzel@ki.si; aljaz.godec@ki.si

Notes

The authors declare no competing financial interest.

ACKNOWLEDGMENTS

We thank U. Maver for his help in preparation of schematics and professors P.G. Debenedetti, M. R. Johnson, M. Gaberšček, and P. Ziherl for suggestions and critical reading of the manuscript.

REFERENCES

- (1) Chandler, D. *Nature* **2005**, *437*, 640.
- (2) Lum, K.; Chandler, D.; Weeks, J. D. *J. Phys. Chem B* **1999**, *103*, 4570.
- (3) Rajamani, S.; Truskett, T. M.; Garde, S. *Proc. Natl. Acad. Sci. U.S.A.* **2005**, *102*, 9475.
- (4) Mittal, J.; Hummer, G. *Proc. Natl. Acad. Sci. U.S.A.* **2008**, *105*, 20130.
- (5) Huang, D. M.; Chandler, D. *Proc. Natl. Acad. Sci. U.S.A.* **2000**, *97*, 8324.
- (6) Papoian, G. A.; Ulander, J.; Eastwood, M. P.; Luthey-Schulten, Z.; Wolynes, P. G. *Proc. Natl. Acad. Sci. U.S.A.* **2004**, *101*, 3352.
- (7) Rabani, E.; Reichman, D. R.; Geissler, P. L.; Brus, L. E. *Nature* **2003**, *426*, 271.
- (8) Stillinger, F. H. *Science* **1980**, *20*, 451.
- (9) Garde, S.; Patel, A. J. *Proc. Natl. Acad. Sci. U.S.A.* **2011**, *108*, 16491.
- (10) Murthy, K. P.; Privalov, P. L.; Gill, S. J. *Science* **1990**, *247*, 559.
- (11) Lynden-Bell, R. M.; Giovambattista, N.; Debenedetti, P. G.; Head-Gordon, T.; Rossky, P. J. *Phys. Chem. Chem. Phys.* **2011**, *13*, 2748.
- (12) Pratt, L. R. *Rev. Mod. Phys.* **2006**, *78*, 159.
- (13) Hummer, G.; Garde, S.; Garcia, A. E.; Pohorille, A.; Pratt, L. R. *Proc. Natl. Acad. Sci. U.S.A.* **1996**, *93*, 8951.
- (14) Tanford, C. *Science* **1978**, *200*, 1012.
- (15) Ben-Naim, B. *Hydrophobic Interactions*; Plenum: New York, 1980.
- (16) Pratt, L. R. *Annu. Rev. Phys. Chem.* **2002**, *53*, 409.
- (17) Bowron, D. T.; Filipponi, A.; Roberts, M. A.; Finney, J. L. *Phys. Rev. Lett.* **1998**, *81*, 4164.
- (18) Chatterjee, S.; Debenedetti, P. G.; Stillinger, F. H.; Lynden-Bell, R. M. *J. Chem. Phys.* **2008**, *128*, 124511.
- (19) Mahoney, M. W.; Jorgensen, W. L. *J. Chem. Phys.* **2000**, *112*, 8910.
- (20) Berendsen, H. J. C.; Grigera, J. R.; Straatsma, T. P. *J. Phys. Chem.* **1987**, *91*, 6269.
- (21) Underwood, R.; Ben-Amotz, D. *J. Chem. Phys.* **2011**, *135*, 201102.
- (22) Laage, D.; Hynes, J. T. *Science* **2006**, *311*, 832.
- (23) Godec, A.; Smith, J. C.; Merzel, F. *Phys. Rev. Lett.* **2011**, *107*, 267801.
- (24) Rossky, P. J.; Karplus, M. *J. Am. Chem. Soc.* **1979**, *101* (101), 1913.
- (25) Turner, J.; Soper, A. K. *J. Chem. Phys.* **1994**, *101*, 6116.
- (26) Sidhu, K. S.; Goodfellow, J. M.; Turner, J. Z. *J. Chem. Phys.* **1999**, *110*, 7943.
- (27) Fidler, J.; Rodger, P. M. *J. Phys. Chem. B* **1999**, *103*, 7695.
- (28) Silvestrelli, P. L. *J. Phys. Chem. B* **2009**, *113*, 10728.
- (29) Rossato, L.; Rosseto, F.; Silvestrelli, P. L. *J. Phys. Chem. B* **2012**, *116*, 4552.
- (30) Perera, P. N.; Fega, K. R.; Lawrence, C.; Sundstrom, E. J.; Tomlinson-Phillips, J.; Ben-Amotz, D. *Proc. Natl. Acad. Sci. U.S.A.* **2009**, *106*, 12230.
- (31) Laage, D.; Hynes, J. T. *J. Phys. Chem. B* **2008**, *112*, 14230.
- (32) Eaves, J. D.; Loparo, J. J.; Fecko, C. J.; Roberts, S. T.; Tokmakoff, A.; Geissler, P. L. *Proc. Natl. Acad. Sci. U.S.A.* **2005**, *102*, 13019.
- (33) Laage, D. *J. Phys. Chem. B* **2009**, *113*, 2684.
- (34) Moilanen, D. E.; Wong, D.; Rosenfeld, D. E.; Fenn, F. E.; Fayer, M. D. *Proc. Natl. Acad. Sci. U.S.A.* **2009**, *106*, 375.
- (35) Ji, M.; Odelius, M.; Gaffney, K. J. *Science* **2010**, *328*, 1003.

- (36) Laage, D.; Stirnemann, G.; Sterpone, F.; Rey, R.; Hynes, J. *Annu. Rev. Phys. Chem.* **2011**, *62*, 395.
- (37) Tatini Titantah, J.; Karttunen, M. *J. Am. Chem. Soc.* **2012**, *134*, 9362.
- (38) Wallace, D. C. *Phys. Rev. A* **1989**, *39*, 4843.
- (39) Gillespie, D. T. *Am. J. Phys.* **1983**, *51*, 520.
- (40) Ben-Amotz, D.; Underwood, R. *Acc. Chem. Res.* **2008**, *41*, 957.
- (41) Irudayam, S. J.; Henschman, R. H. *J. Phys.: Condens. Matter* **2010**, *22*, 284108.
- (42) Gu, S. J.; Sun, C. P.; Lin, H. Q. *J. Phys. A: Math. Theor.* **2008**, *41*, 024002.
- (43) Qvist, J.; Halle, B. *J. Am. Chem. Soc.* **2008**, *130*, 10345.
- (44) Graziano, G. *J. Chem. Phys.* **2004**, *121*, 1878.
- (45) Soper, A. K.; Benmore, C. J. *Phys. Rev. Lett.* **2008**, *101*, 065502–1.
- (46) Rogers, D. M.; Beck, T. L. *J. Chem. Phys.* **2010**, *132*, 014505.
- (47) Laage, D.; Stirnemann, G.; Hynes, J. *J. Phys. Chem. B* **2009**, *113*, 2428.